



Endoscopy video analysis algorithms and their independence of rotation, brightness, contrast, color and blur

Jan Cychnerski

Department of Computer Architecture, Gdańsk University of Technology, Poland

ABSTRACT: The article presents selected image analysis algorithms for endoscopy videos. Mathematical methods that are part of these algorithms are described, and authors' claims about the characteristics of these algorithms, such as the independence of rotation, brightness, contrast, etc. are mentioned. Using the common test on the real endoscopic image database and a set of image transformations, the validity of these claims was checked and compared between algorithms. Many of the results seem to differ from the declaration of the authors, sometimes even strongly denying them. In addition, some algorithms were found extraordinary sensitive to blurring of the images, which indicates the possibility of using them for the detection of blurry frames, not just diseases.

KEYWORDS: endoscopy, video analysis, independence, rotation, brightness, contrast, color, blur

I. INTRODUCTION

In the past several years, endoscopic movie analysis algorithms (obtained by gastroscopy, colonoscopy or capsule endoscopy) were gaining popularity. These algorithms are used to recognize informative and non-informative frames, and various diseases or healthy tissues. Unfortunately, the algorithms described in the literature do not have any larger comparative tests, which makes a comparison between them almost impossible. In addition, the authors of mathematical methods used in these algorithms do not provide evidence for their claims (e.g. on the algorithms' independence of transformations such as rotation or brightness change). [1]

This article focuses on a comparison of selected endoscopic image analysis algorithms and mathematical tools used in them. The algorithms were tested with a special comparator to check if their authors' claims about the independence of image transformations like rotation, brightness, contrast, blur and color change are trustworthy.

II. TEST PROCEDURE

All tests were carried out on a common database of real colonoscopy videos [2]. For the tests, 100 random images from the database were selected. The algorithms' classification part was removed, leaving only the kernel of the algorithms - the calculation of the feature vectors. In the next step, every feature was normalized so that the average (calculated over all the images in the database) was equal to 0 and standard deviation to 1.

Only the normalized feature vectors were analyzed in the article (ignoring the classification component, such as neural networks or support vector machines). In the literature it is often claimed that the algorithms are dependent or independent of the various image transformations. For comparison and test purposes, 5 popular transformations that occur naturally in endoscopy were selected, as in table I.

A. Comparison measure

In the first place, feature vectors from original images were compared with each other using the metrics described below.

Let $F(a)$ be a feature vector of image a for algorithm F , and $f_i(a)$ be its i -th normalized value:

International Journal of Innovative Research in Computer and Communication Engineering

(An ISO 3297: 2007 Certified Organization)

Vol. 2, Issue 8, August 2014

Table I: Image transformations

| ID | Transform | Description | Values |
|----|------------|--|----------------------|
| 1 | brightness | Change of brightness by a multiplying factor | 1.3 – 2 or 0.5 – 0.8 |
| 2 | Contrast | Change of contrast by a multiplying factor | 1.2 – 2 or 0.5 – 0.8 |
| 3 | Color | Change of pixels' hue and saturation | ± 20 – 301 |
| 4 | Rotation | Rotation of the image from its center | 45° – 315° |
| 5 | Blur | Box filter blur | Kernel size 3 – 7 |

$$F(a) = [f_1(a), f_2(a), \dots]$$

To obtain a common comparing base for algorithm F , feature vectors of all original images (a, b, c, \dots) were compared with each other. Then, the average base feature difference was calculated as follows::

$$d_i(a, b) = \begin{cases} 0 & \text{if } f_i(a) = f_i(b) = 0 \\ \frac{|f_i(a) - f_i(b)|}{\max(|f_i(a)|, |f_i(b)|)} & \text{otherwise} \end{cases}$$

$$D_0 = \text{mean}(d_i(a, b) \text{ for each } i, a, b, \text{ where } a \neq b)$$

$$\sigma_0 = \text{std.dev.}(d_i(a, b) \text{ for each } i, a, b, \text{ where } a \neq b)$$

The difference between the feature vector between original and transformed images was defined analogously, with additional normalization in regard of typical not-transformed image feature vector differences:

$$T(a) = \text{image } a \text{ modified with transform } T$$

$$D_T = \frac{\text{mean}\{d_i(a, T(a)) \text{ for each } i, a\}}{D_0}$$

$$\sigma_T = \frac{\text{std.dev.}\{d_i(a, T(a)) \text{ for each } i, a\}}{\sigma_0}$$

III. MATHEMATICAL OPERATIONS

In this section, mathematical operations used in the analyzed algorithms are described. Most of them focus on the spatial features of the images, brightness changes and edge detection. This is due to the fact that these features are similar to human vision methods of seeing objects, which allows humans to recognize textural anomalies in the image. Some transformations, however, focus more on the color features, as they are the second most characteristic phenomenon differentiating healthy tissue from cancer (e.g. shades of gray, black or bright red are found almost only in cancerous tissue).

Most of the algorithms include also some form of statistical analysis of the characteristics of the image. Depending on the analyzed image features, this allows to reduce the number of dimensions of the resulting feature vector or make it independent from the scale, rotation, or change of contrast or brightness of the image.

Some of the transformations are commonly known in the field of image analysis (e.g. Gabor filters or discrete wavelet transforms), but some are designed specifically for endoscopic (e.g. AHT, N_{TU}).

Table III provides information about the chosen algorithms for the analysis of endoscopy videos provided by the authors (rot. = rotation, sca. = scale, bri. = brightness, con. = contrast).

International Journal of Innovative Research in Computer and Communication Engineering

(An ISO 3297: 2007 Certified Organization)

Vol. 2, Issue 8, August 2014

Table II: Mathematical operations

| Ref. | Operation | Description | Rot. | Bri. | Con. |
|------|---|--|------|------|------|
| | pixel value quantization | data dimension reduction | | | |
| | histograms | statistical features of the data | ✓ | | |
| | colorspace change | matching color spaces to match human vision | | | |
| [17] | Local Binary Pattern (LBP) | grayscale local texture pattern numbering | | ✓ | ✓ |
| [16] | Texture Unit Number (N_{TU}) | similar to LBP, but slightly generalized | | ✓ | ✓ |
| [18] | Multi-scale Block LBP (MB-LBP) | block LBP (pixels in blocks are averaged or blurred) | | ✓ | ✓ |
| [6] | Rotation Independent Uniform LBP (LBP_{PR}^{nu2}) | rotation-independent LBP; texture homogeneity assumed | ✓ | ✓ | ✓ |
| [10] | Local Color Vector Pattern (LCVP) | similar to LBP, but for color images | | | |
| [19] | Canny Edge Detector | grayscale edge detection, based on sharp brightness change | ✓ | ✓ | |
| [20] | Gray-Level Coocurrence Matrices (GLCM) | spatial dependencies of pixels | | ✓ | ✓ |
| | Discrete Cosine / Transform (DCT) | conversion from raster image to frequency domain | | ✓ | |
| | Discrete Fourier Transform (DFT) | conversion from raster image to frequency domain | | ✓ | |
| | Discrete Wavelet Transforms (DWT) | multi-scale frequency-like transforms | | | |
| [9] | Color Wavelet Covariance (CWC) | variance and covariance from coocurrence matrices of DWT | | | |
| [21] | Gabor Filters | directional image filters (mainly for edge detection) | | ✓ | |
| [22] | Simple Gabor Feature Space (SGFS) | set of gabor filters for specific scales and directions | | ✓ | |
| [3] | Autocorrelation Gabor Feature (AGF) | rotation and scale-independent SGFS | ✓ | ✓ | |
| [4] | Homogeneous Texture (HT) | statistics of SGFS for every given direction and scale | | ✓ | |
| [3] | Autocorrelation Homogeneous Texture (AHT) | statistics of AGF | ✓ | ✓ | |

IV. TEST RESULTS

The following figures present the results of tests carried out. Figure 1 shows the differences between the untransformed images, i.e. D_0 and σ_0 . Figures 2 – 6 present: differences after brightness change $D_{\text{brightness}}$, after contrast change D_{contrast} , after color change D_{color} , after rotation D_{rotation} and after blurring D_{blur} .

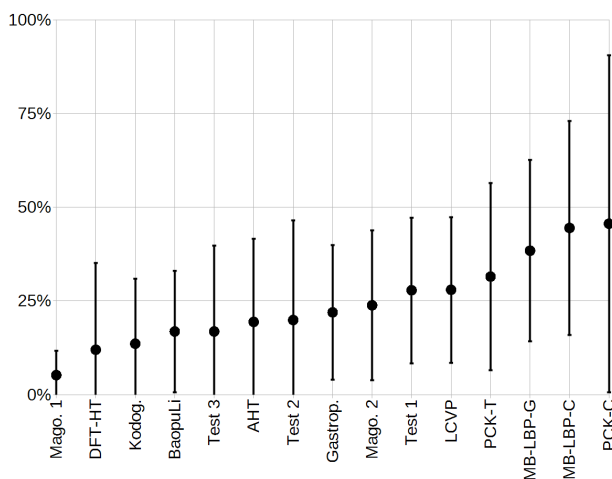


Figure 1: Untransformed images difference D_0

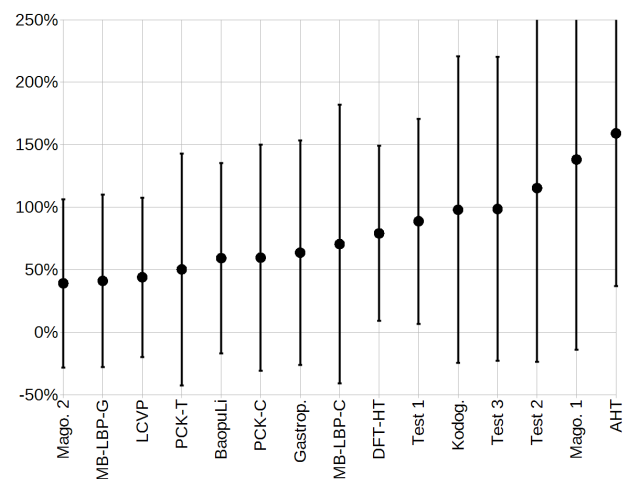


Figure 2: Differences after brightness change $D_{\text{brightness}}$

International Journal of Innovative Research in Computer and Communication Engineering

(An ISO 3297: 2007 Certified Organization)

Vol. 2, Issue 8, August 2014

Table III: Algorithms' characteristics

| Ref. | Algorithm | ID | Objects detected | Color spaces | Independence of | | | | | Components | Feature vector |
|------|--|----------|---|-------------------|-----------------|-----|-----|-----|-----|---|---|
| | | | | | Rot | Sca | Bri | Con | Hue | | |
| [3] | Autocorrelation Homogeneous Texture | AHT | tumor in chromoendoscopy and narrow-band imaging | gray | ✓ | ✓ | ✓ | | ✓ | Gabor filters, AGF, AHT, SGFS, AHT | AHT |
| [4] | Discrete Fourier Transform – Homogeneous Texture | DFT-HT | textures | gray | ✓ | ✓ | | | ✓ | Gabor filters, SGFS, HT, DFT | HT |
| [5] | Gastropathy | Gastrop. | portal hypertensive gastropathy in gastroscopy | gray, HSV | ✓ | | | | | Canny edge detection, thresholding | % of edge pixels |
| [6] | | | | gray | ✓ | | ✓ | ✓ | ✓ | LBP_{PR}^{riu2} | histogram P+2 bins (only P=16 tested) |
| [7] | | | | gray | ✓ | ✓ | ✓ | ✓ | ✓ | Local Brightness Maximias, thresholding | % of blocks with maximas |
| [8] | Baopu Li | BaopuLi | adenoma, adenocarcinoma in Wireless Capsule Endoscopy (WCE) | RGB, HSI, CIE-Lab | ✓ | | | | | DWT (CDF9/7), LBP | 10-bin histograms for each channel = 630 values |
| [9] | Poh Chee Khun | PCK-C | informative frames, bleeding in WCE | HSV | ✓ | | | | | color quantization (H=12, S=5, V=8), 9 blocks, histograms | hisgoram for each block for each quantized value |
| | | PCK-T | | HSV | ✓ | | ✓ | ✓ | | 2x DWT (9 channels), GLCM (4 statistics), statistics | CWC – 72 features + 8 additional |
| [10] | Local Color Vector Pattern | LCVP | textures in magnification endoscopy | RGB lub CIE-Lab | ✓ | | ✓ | ✓ | ✓ | MB-LBP, LCVP, histogram | histogram of LCVP – 256 – features |
| [11] | Multi-scale Block LBP | MB-LBP-G | patterns for face recognition | GRAY | ✓ | ✓ | | | | MB-LBP, histogram | histogram – 256 features |
| [12] | | MB-LBP-C | polyps in endoscopy | RGB | ✓ | ✓ | | | | discarding one of the channels, MB-LBP, 2D-histogram | 2D-histogram – up to 256 ² features (tested up to 256) |
| [13] | Test | Test 1 | tumor, polyps, informative frames in endoscopy | RGB, HSV | ✓ | ✓ | | ✓ | | mean value for each channel | 6 features |
| | | Test 2 | | RGB, HSV, Lab | ✓ | ✓ | | | | mean, variance, covariance and energy for each channel | 36 features |
| | | Test 3 | | RGB, HSV, Lab | ✓ | ✓ | | | | 10 statistics for each channel | 90 features |
| [16] | Kodogiannis | Kodog. | normal/abnormal tissue in WCE | RGB, HSV | | | ✓ | ✓ | | N_{TU} , 9 statistics for each channel | 54 features |
| [14] | Magoulas | Mago. 1 | normal/abnormal tissue in colonoscopy | GRAY | ✓ | | ✓ | ✓ | ✓ | GLCM for 4 directions, 4 statistics | 16 features |
| [15] | | Mago. 2 | | GRAY | ✓ | | ✓ | ✓ | ✓ | DWT, 4x GLCM, 4 statistics for each | 48 features |

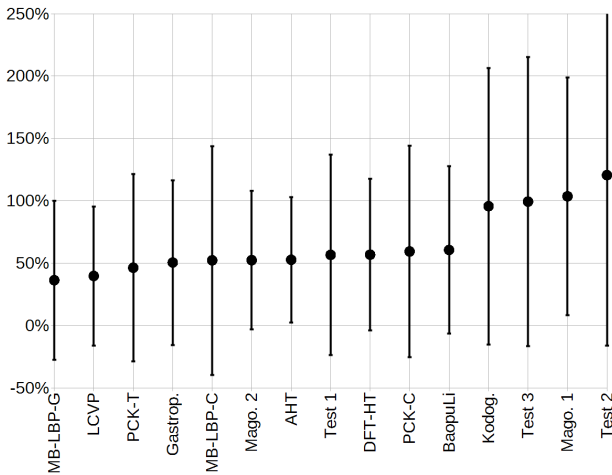


Figure 3: Differences after contrast change $D_{contrast}$

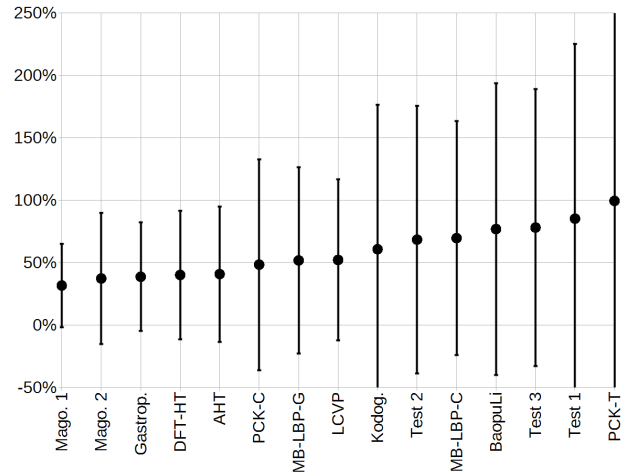


Figure 4: Differences after color change D_{color}

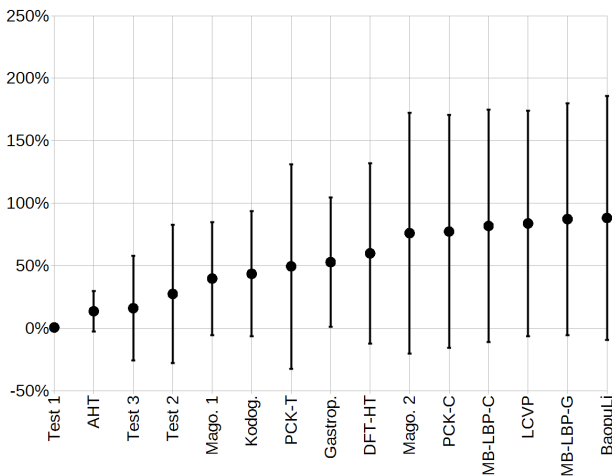


Figure 5: Differences after rotation $D_{rotation}$

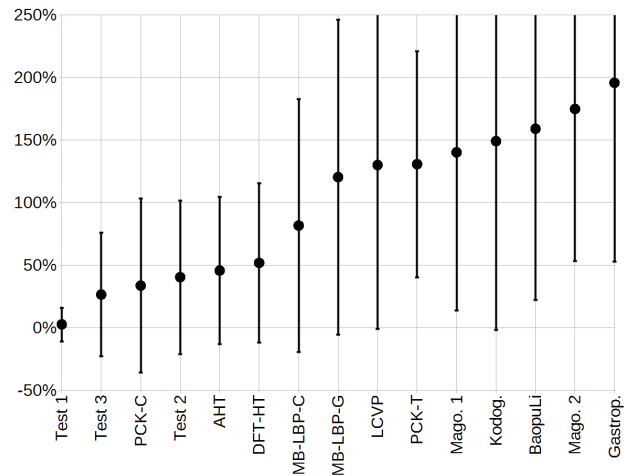


Figure 6: Differences after blurring D_{blur}

V. CONCLUSION

The article presents mathematical tools used in the gastrointestinal endoscopic video analysis algorithms. The tests show that algorithms' authors' claims about some characteristics of their algorithms about independence from the transformations such as rotation, brightness change, etc. does not always comply with the practical results. Moreover, many of the algorithms are surprisingly sensitive to some transformations – in such cases the difference between the transformed images can be greater than that between the other images. This phenomenon questions the usefulness of these algorithms in provided by the authors applications. However, it is worth noting that some of the algorithm are remarkably sensitive to image blur – this fact indicates these algorithms may perform well in the task of blurry frames recognition, which is also useful in systems supporting digestive system diagnosis.

REFERENCES

1. M. Liedlgruber, A. Uhl, Computer-aided decision support systems for endoscopy in the gastrointestinal tract: a review., IEEE reviews in biomedical engineering, vol. 4, pp. 73–88, 2011.



International Journal of Innovative Research in Computer and Communication Engineering

(An ISO 3297: 2007 Certified Organization)

Vol. 2, Issue 8, August 2014

2. J. Cychnerski, A. Brzeski, A. Blokus, T. Dziubich, and M. Jędrzejewski, Konstrukcja bazy danych dla systemu wspomagania diagnostyki chorób przewodu pokarmowego. In: *Studia Informatica*, 2012, vol. 33, no. 1. [in polish]
3. Riaz F., Silva F.B., Dinis Ribeiro M., Coimbra M.T., Invariant Gabor Texture Descriptors for Classification of Gastroenterology Images, *IEEE Transactions on Biomedical Engineering*, vol. 59, no. 10, Październik 2012
4. Riaz F., Hassan A., Rehman S., Qamar U., Texture Classification Using Rotation- and Scale-Invariant Gabor Texture Features, *IEEE Signal Processing Letters*, vol. 20, no. 6, 2013. Manjunath B.S., Ma W.Y., Texture Features for Browsing and Retrieval of Image Data, *IEEE Transactions on Pattern Analysis and Machine Intelligence*, vol. 18, no. 8, 1996
5. P. Dorożyński, T. Dziubich, Ocena możliwości zautomatyzowanej analizy obrazów z badań endoskopowych do wspomagania diagnostyki gastropatii wrotnej. Materiały konferencyjne ICT Young 2012, p. 341-348 [in polish]
6. Ojala T., Pietikainen M., Maenpaa T., Multiresolution Gray-Scale and Rotation Invariant Texture Classification with Local Binary Patterns, *IEEE Transactions on Pattern Analysis and Machine Intelligence*, vol. 24, no. 7, 2002
7. J. Cychnerski, P. Dorożyński, T. Dziubich. An algorithm for portal hypertensive gastropathy recognition on the endoscopic recordings. *Information Systems Architecture and Technology*, No. 35, 2014.
8. Li B., Meng M. Q.-H., Tumor Recognition in Wireless Capsule Endoscopy Images Using Textural Features and SVM, *IEEE Transactions On Information Technology In Biomedicine*, vol. 16, no. 3, 2012
9. Poh Chee Khun, Zhang Zhuo, Liang Zi Yang, Li Liyuan, Liu Jiang, Feature Selection and Classification for WirelessCapsule Endoscopic Frames, *Biomedical and Pharmaceutical Engineering.. ICBPE '09. International Conference, 2009*
10. Häfner M., Liedlgruber M., Wrba F., Uhl A., Vecsei A., Color treatment in endoscopic image classification using multi-scale local color vector patterns, *Medical Image Analysis*, 16(1): 75–86, January 2012
11. Liao S., Zhu X., Lei Z., Zhang L., Li S. , Learning multi-scale block local binary patterns for face recognition, *Advances in Biometrics*; pp. 828–837, 2007
12. Häfner M., Gangl A., Liedlgruber M., Uhl A., Vecsei A., Wrba F., Pit Pattern Classification using Extended LocalBinary Patterns, In: *Proceedings of the 9th International Conference on Information Technology and Applications in Biomedicine (ITAB'09)*, Larnaca, Cyprus., 2009
13. A. Brzeski, J. Cychnerski, Rozpoznawanie chorób układu pokarmowego z wykorzystaniem technik sztucznej inteligencji, in: *Zeszyty Naukowe Wydziału Elektroniki, Telekomunikacji i Informatyki Politechniki Gdańskiej.*, 2011, no. 9, pp. 395–400. [in polish]
14. G.D. Magoulas, V.P. Plagianakos, oraz M.N. Vrahatis. Neural networkbased colonoscopic diagnosis using on-line learning and differential evolution. *Applied Soft Computing*, 2004
15. G.D. Magoulas. Neuronal networks and textural descriptors for automated tissue classification in endoscopy. *Oncology Reports*, 15, 2006.
16. V.S. Kodogiannis oraz M. Boulougoura. An adaptive neurofuzzy approach for the diagnosis in wireless capsule endoscopy imaging. *International Journal of Information Technology*, 13(1), 2007
17. T. Ojala, M. Pietikäinen, and D. Harwood (1994), "Performance evaluation of texture measures with classification based on Kullback discrimination of distributions", *Proceedings of the 12th IAPR International Conference on Pattern Recognition (ICPR 1994)*, vol. 1, pp. 582 - 585.
18. Liao S., Zhu X., Lei Z., Zhang L., Li S. , Learning multi-scale block local binary patterns for face recognition, *Advances in Biometrics*; pp. 828–837, 2007
19. Canny, J., A Computational Approach To Edge Detection, *IEEE Trans. Pattern Analysis and Machine Intelligence*, 8(6):679–698, 1986.
20. R.M. Haralick, K. Shanmugam, oraz I. Dinstein. Textural features for image classification. *IEEE Transactions on systems, man, and cybernetics*, November 1973
21. Wu P., Manjunath B.S., Newsam S., Shin H.D., A texture descriptor for browsing and similarity retrieval, *Elsevier, Signal Processing: Image Community*, vol. 16, no. 1, 2000
22. Kamarainen J.-K., Kyrki V., Kälviäinen H., Invariance Properties of Gabor Filter-Based Features-Overview and Applications, *IEEE Transactions on Image Processing*, vol. 15, no. 5, Maj 2006